An Effort to Replace Interior Permanent Magnets Rotors with Assisted Reluctance Rotors

Konstantinos Ntontis
Technical University of Cluj Napoca
Cluj Napoca, Romania
Konstantinos.Ntontis@mae.utcluj.ro

Claudia Steluta Martis
Technical University of Cluj Napoca
Cluj Napoca, Romania
claudia.martis@emd.utcluj.ro

***Abstract*— The scarcity and increasing price of rare earth magnets, forces researchers to design permanent magnet machines with a smaller volume of rare earth magnets. The aim of this paper is to propose and analyze a PM-less machine with respect to an interior permanent magnet synchronous machine (IPMSM). The IPMSM considered as reference machine in this paper is used in assisted power steering systems in the automotive industry. The proposed topology has the same stator (lamination, cross-section) and a rotor with flux barriers and permanent magnets.**

Keywords—Permanent magnet assisted synchronous reluctance machine, interior permanent magnet machine, torque ripple, IPMSM, PMaSynRM.

I. Introduction

Interior Permanent Magnet Synchronous Machines (IPMSM) have been proven to have a wide constant power – speed range operation and a high-power density [1]. The main drawback of this type of machines is the use of rare earth permanent magnets as they are constructed from critical raw materials [2]. An alternative solution for applications such as the assisted power steering could be a Permanent Magnet Assisted Synchronous Reluctance Motor (PMaSynRM). A PMaSynRM is an IPMSM that has a higher magnetic anisotropy and makes use of less PM. Due to the magnetic anisotropy, the PMaSynRM has two torque components: the synchronous (PM) and the reluctance torque, respectively. The added reluctance torque (due to rotor anisotropy) allows for a reduction in the volume of PMs. Nevertheless, there are some drawbacks like higher torque ripple and iron losses, vibrations and mechanical constraints [3].

The aim of this paper is to analyze and propose a PM-less machine, by reducing the PM volume and increasing the reluctance torque component. In the proposed PMaSynRM topology, it is applied the same stator lamination cross section as for the IPMSM. The winding and the rotor of the PMaSynRM will be designed and optimized in order to achieve the performance of the reference motor. Torque ripple is an important issue in the proposed solution as the number of poles is decreasing. Iron losses and vibrations are not to be considered in this study, but mechanical constraints are important because the electromagnetic optimization is done on the degradation of the rotor's mechanical robustness [4].

II. Reference Machine

The reference machine is an IPMSM used in the automotive industry for electric assisted power steering systems (Fig. 1). The machine is a 12 slot/10 pole one, equipped with concentrated windings and NdFeB magnets. The volume of the PMs is equal to 20880 mm^3.

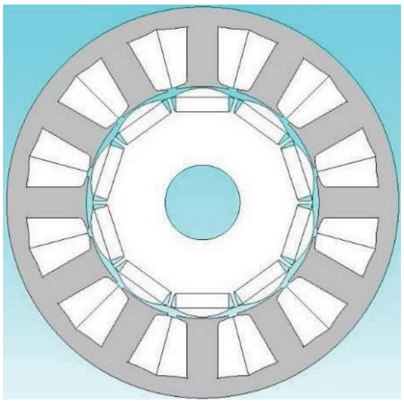

Fig. 1 Cross-section of the reference machine

Table I summarizes the most significant specifications of the reference machine.

TABLE I. Reference machine's parameters

Parameter	**Value**	**Unit**
Power	0.8	kW
DC-Bus voltage	12	V
Phase resistance	0.0069	Ω
Base speed	1000	rpm
Core Material	M330-50A	
Magnet type	NdFeB 1.4	T
Number of slots	12	
Stack length	58	mm
Number of poles	10	

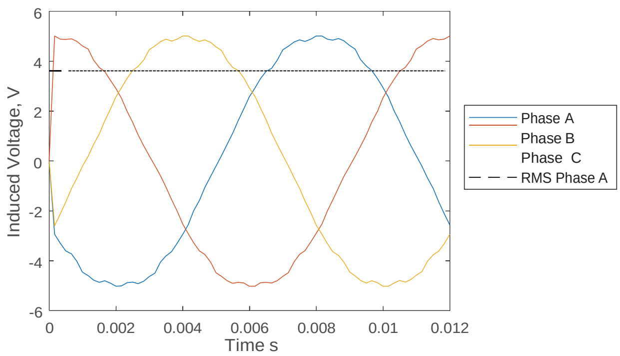

Fig. 2 Induced electromotive force for the reference machine working as generator at no-load

The electromagnetic analysis of the reference machine provides: (i) the induced electromagnetic force for the machine (when working as a generator at no-load and rated speed) (ii) the rated electromagnetic torque, and (iii) the magnetic field distribution in the cross-section. All these are depicted in Fig. 2 to 4.

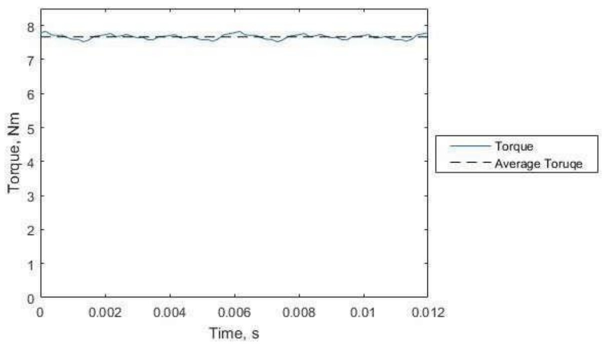

Fig. 3 Electromagnetic torque developed by the reference machine at rated speed

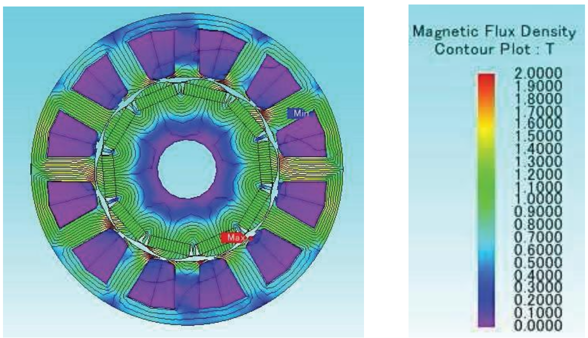

Fig. 4 Magnetic flux distribution in the cross section of the reference machine at rated speed

The average value of the electromagnetic torque at rated speed is 7.66 Nm, with a ripple content of 4%.

III. PM-LESS SYNCHRONOUS MACHINE

In order to reduce the amount of rare earth PMs, a topology based on the combination of synchronous and reluctance torque is proposed. Thus, based on previous research work [5] a PMaSynRM topology with the same cross-section of the stator and with a four-pole rotor was designed and analyzed.

A. PMaSynRM electromagnetic torque

The electromagnetic torque of a PMaSynRM is given by:

$$T_{ePWaSynRW} = \frac{3P}{4}\left[L_d I_d I_q - (L_q I_q + \lambda_m) I_d\right]$$
$$= \frac{3P}{4}\left[(L_d - L_q) I_d I_q - \lambda_m I_d\right] \quad (1)$$

where λ_m is PM flux linkage, P is the number of poles and L_d, L_q, I_d , I_q are the inductances and the currents in the d and q axis respectively. It can be noticed that the second term of Eq. (1) is negative. Thus, the direction of the produced flux linkage from the magnets is oriented in such a way as to oppose and eliminate this negative contribution. In other words, the PM flux linkage ideally could be equal with the flux linkage produced by the stator currents in the q axis [6]. Theoretically, the PM flux linkage can be obtained by ferrite magnets since the value of L_q is low. Moreover, the increase in difference between L_d and L_q and the increase in ratio L_d/L_q could improve the torque density and power factor [7]. The Eq. (1) is also valid for an IPMSM but with an alternation; the current in the second term must be changed with the q axis current because the ‘dq' reference frame is used differently.

B. PMaSynRM rotor design

The rotor of the initial proposed machine (Fig. 5) is designed with air cavities perpendicular to the q axis and side air cavities horizontal to the d axis. The air cavities perpendicular to the q axis are there to host the permanent magnets and for enhancing the production of reluctance torque. As it can been seen from Eq. (1) the larger the difference between the two inductances the greater will be the reluctance torque component.

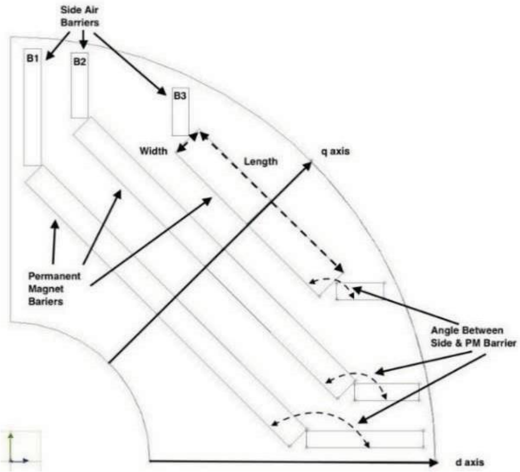

Fig. 5. Initial proposed rotor design

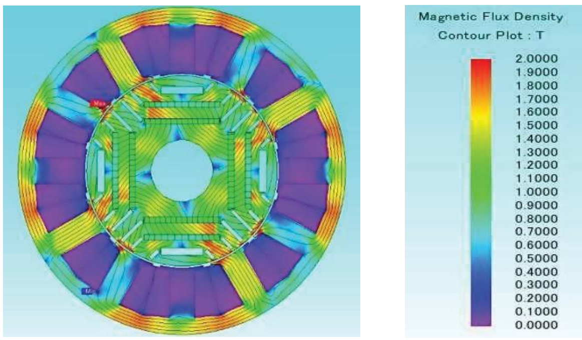

Fig. 6. Magnetic flux density of the initial proposed design

This difference can be obtained by minimizing the q axis inductance and maximizing the d axis inductance. The L_q inductance is minimized by means of the introduced barriers (perpendicular air cavities to the q axis) because the produced flux lines from the stator windings are facing a greater magnetic reluctance. On the other side, L_d inductance is maximized when the corresponding flux lines are able to pass through the rotor without producing saturation. From the above description it is clear that the reluctance torque is maximized when the rotor is positioned in such a way that the reluctance seen by the armature flux is increasing.

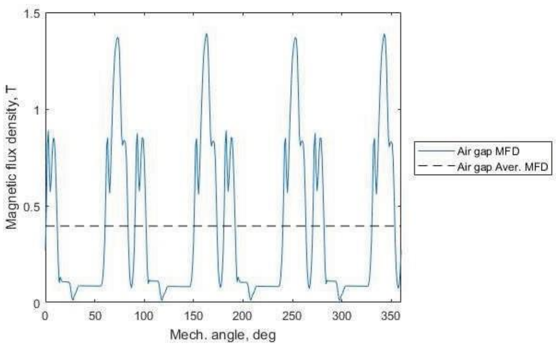

Fig. 7. Absolute air gap magnetic flux density for the initial proposed design

Side air cavities prevent flux lines, generated by the magnets, to flow to the opposite magnetized poles and force them to pass through the air gap. This configuration has two effects: it prevents the rotor yoke from being saturated and it contributes to the maximization of the reluctance torque. When the permanent magnets' flux is concentrated on the q axis the magnetic field density is more (more flux lines in the same area) and this makes the difference between L_d and L_q larger. Another use of the side air cavities is the limitation of the torque pulsations. This can be achieved when each air cavity has different angle with respect to the corresponding perpendicular - to q axis - air cavity (Fig. 5). This aspect will be explained in more detail in Section IV.

The reference machine has been constructed with sintered NdFeB. This kind of rare earth magnets have high remanence (B_r), high energy product (BH_{max}) but on the other side they have a high price and low Curie temperature at 310-400 L [8]. Ferrite magnets on the other hand have excellent resistance to demagnetization and to corrosion and their working temperature could be up to 250 L. Besides that, they have high electrical resistivity. Their drawback is that they have low remanence, around 0.4 T in contrast with the NdFeB magnets that have a maximum remanence of 1.4 T [9]. Therefore, NdFeB magnets have been finally chosen for the proposed PMaSynRM.

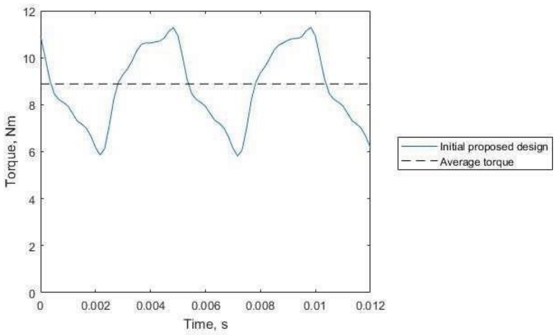

Fig. 8. Torque of the initial proposed design

The rotor in Fig. 5 provides an average torque of 8.88 Nm but with a torque ripple rate of 61.5% (Fig. 8). The simulation carried out with 155.56 Apeak and a 19680 mm^3 volume of magnets. The average electromagnetic torque is over the targeted torque (7.66 Nm) but the torque ripple rate is unacceptable for this application. In order to eliminate the torque pulsation an optimization algorithm - Multi Objective Genetic Algorithm (MOGA) -that can combine the maximization of the average torque and in the same time the minimization of the torque ripple was implemented. The rotor's dimensions that were optimized are i) the length and the width of the cavities, ii) the distance between shaft and 1st barrier, iii) the distance between the barriers and lastly iv) the angle between the side air cavities and the cavities which host the magnets. Of course, more dimensions must be changed/optimized like the distance between the side air cavities and the magnetic pole border. In the optimization process some of these dimensions are kept constant (because their optimal values had already been found) or other were changed automatically (their values were dependent on equations) in such a way so the resulted rotor design was valid.

The cavities' curved edges and the absence of the side air cavities in the third flux barrier (Fig. 10) is the result of mechanical robustness limitations and torque ripple reduction correspondingly. Furthermore, the magnets' volume of the new rotor not only should not exceed the magnets' volume of the reference machine but it must be smaller than that. Fig. 9 depicts the results of the optimization (Pareto Curve). Finally, the optimum rotor topology presented in Fig. 10 provides 7.81 Nm average electromagnetic torque and a 13.04% ripple content. The magnets' volume of the optimized rotor is 15744 mm^3. There is a reduction of 24.6% of NdFeB and an increase of 41% in the active axial length of the machine compared to the reference machine (the axial length is also increased in the initial proposed rotor).

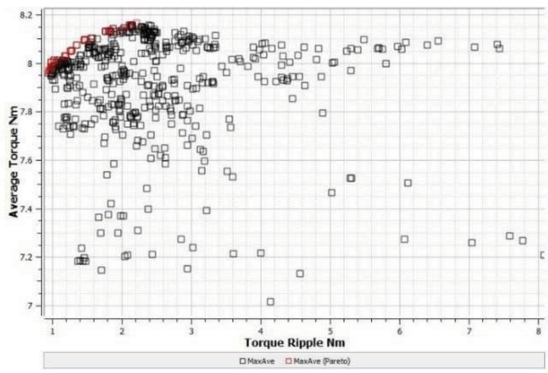

Fig. 9. Optimization's results

Magnetic field distribution across the cross-section of the machine and the absolute airgap magnetic field density for the optimized machine are depicted in Figs. 11 and 12.

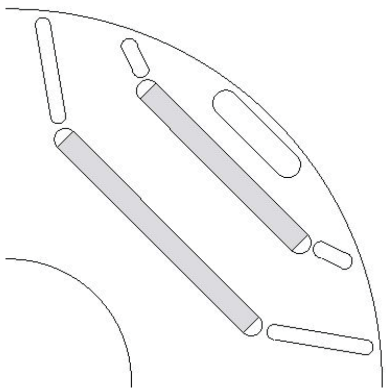

Fig. 10. Optimized rotor design

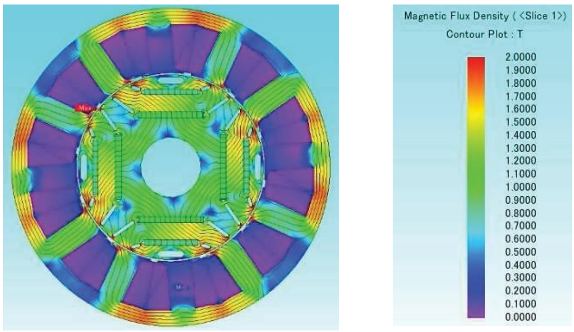

Fig. 11. Magnetic flux density of the optimized design

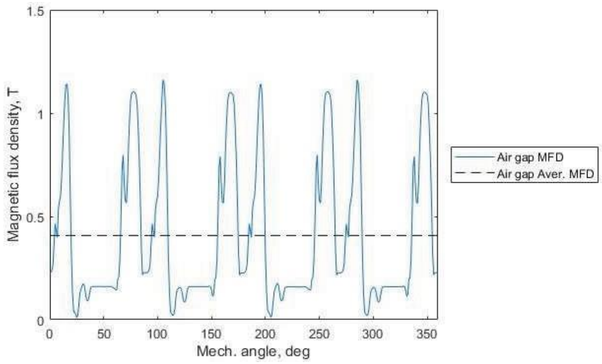

Fig. 12. Air gap magnetic flux density of the optimized machine

The torque ripple content (13.04%) is still not compatible with the targeted application. It is obvious that the first proposed rotor design (Fig. 5) has been altered especially regarding the third barrier (B3). This flux barrier has a significant role in reducing the torque ripple content among others (angle of side air cavities, distance between barriers, etc.). All these design parameters were optimized but the ripple content still must be reduced.

Table II presents the average airgap magnetic flux density, the average electromagnetic torque and the torque ripple content before and after optimization (initial proposed rotor and optimized rotor after skewing has been applied).

TABLE II. AVERAGE AIRGAP MAGNETIC FLUX DENSITY, THE AVERAGE ELECTROMAGNETIC TORQUE AND THE TORQUE RIPPLE CONTENT BEFORE AND AFTER OPTIMIZATION

	B_g [T]	**T [Nm]**	**Torque ripple [%]**
Initial design	0.395	8.88	61.5
Optimized skewed design	0.406	7.61	4.8

IV. TORQUE PULSATIONS REDUCTION

As has been noticed so far from the previous analysis for the proposed rotor, the torque pulsation is a major problem. The torque ripple is due to the interaction between spatial harmonics produced from the magnetomotive force in the stator and the air gap permeance. Cogging torque, on the other hand, occurs from the interaction between PM in the rotor and the stator slots [10]. It is not possible for all the orders of the harmonics to be eliminated or to be canceled out [11]. The best practice is to cancel out one order of harmonic and to lessen the remaining order of harmonics. The design parameters which influence the harmonics' amplitude are: the number of rotor flux barriers, the volume and the positioning of PMs and the insulation ratio in the d and q axis.

In bibliography it can been found different ways for reducing the torque ripple. One of them refers to selecting the appropriate number of flux barriers and stator slots [11]. In this case the angle of the side air cavities must be aligned with the stator's slots. There is a more practical rule which is described in [12]. This rule states that the rotor barriers should be designed in such a way that when one end of the barrier is located under a stator's slot the other end of the same barrier must be placed under a stator's tooth. In [11] it is also proposed the use of different geometry of flux barriers in each pole pair. This rotor configuration is known as “Machaon” and the end barriers angle is not the same for each pole pair.

When the design parameters have been optimized with the help of a Finite Element Analysis tool and the torque pulsation is still not acceptable for the specific application then other solutions must be applied. One of these solutions is to implement stator slot skewing. In [10] it is stated that skewing can be applied both to the rotor or to the stator. Skewing reduces cogging torque because the interaction between the PMs and the slots occurs in an inclined way. Of course, this makes the winding a little longer, its resistance becomes larger and the efficiency of the machine decreases slightly. In addition to this reduction in the efficiency the production cost also increases. Another way of reducing torque pulsation is the magnet segmentation [13]. In order the cogging torque to be sufficiently reduced the number of the magnet segments must be high. Less segments means worse results. Also, this method increases the pole flux leakage. Lastly, teeth notching is not so effective especially for the integer slot stators. The proposed method for eliminating the cogging torque and the torque ripple is according to [13] stator teeth notching for a PMaSynRM. As it has already been stated in this paper the stator must remain attached so this method cannot be implemented.

In [14], [15] it is proposed an equation for calculating the angle of skewing. The cogging torque period N_{period} is obtained from Eq. (2). Where HSF is the Highest Common Factor and S is the number of slots.

$$N_{period} = \frac{P}{HSF\{S, P\}} \tag{2}$$

$$\&_{ckewing} = \frac{360}{S \times N_{period}} \tag{3}$$

The author of this paper [14] concludes that the best cogging torque method reduction comparing to a spoke-type IPM machine is rotor pole axial pairing technique. Nevertheless, the reference machine in this study is not a spoke type IPM machine and skewing technique has better results among other applied techniques for cogging torque reduction as described in [14].

The rotor of the initial proposed PMaSynRM was designed after researching for the appropriate number of air cavities for minimizing the torque pulsation and at the same time having the same or a better average torque. The next stage included the optimization of the design parameters with the help of JMAG. The use of different angles for each flux barrier end contributed to the minimization of torque pulsation. Of course, the area of the stator's slots and teeth are not comparable with the rotor's slots area. A stator with more slots and as a consequence a slot and tooth area closer to that of the rotor's slots area could have given better results in terms of torque pulsation.

V. Results analysis

The previous paragraph analyses in short, the methods that can be applied to lower the torque pulsation. However, in order to obtain the same torque ripple as the reference machine, Step skewing has been used. JMAG simulation software provides three ways of skewing: Linear, Step and V-skew. Among them the best is Step skewing at least for this kind of motors (PMaSynRM). The results from the other two types of skewing could not provide a low torque ripple and at the same time a high average torque. It is also worth pointing out that the average torque of the skewed rotor - when a 10° angle and 4 steps were used with Step skewing - it has been reduced but almost has the same average value as with the average torque of the optimized rotor – average value of not skewed torque 7.74 Nm and average value of skewed torque 7.66 Nm (Fig 13).

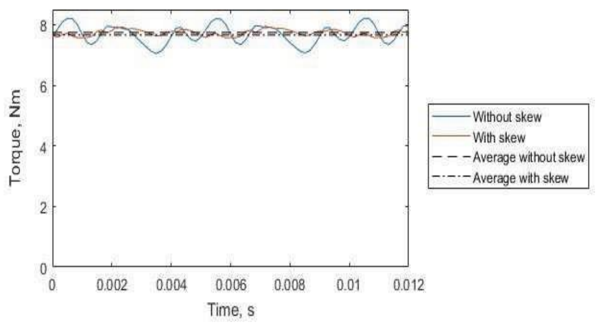

Fig 13. Optimized rotor with and without skewing

Fig. 14 depicts a comparison between reference machine's torque and the chosen skewed case (10° - the skewing angle) at rated speed. The average torque of the skewed case (optimized skewed proposed machine) is not the same as in Fig. 13. A reduction in peak source current was selected (152 A peak) for the torque ripple of the optimized skewed proposed machine to be almost the same as the one from the reference machine. The skewed case average torque is 7,61 Nm and with a 4,8% ripple content. These values are almost the same with the reference's machine average torque and ripple content (7.64 Nm and 4%). Additionally, must be noticed that the skewing simulation and the optimization of the proposed machine were conducted at rated speed and current (155.56 A peak).

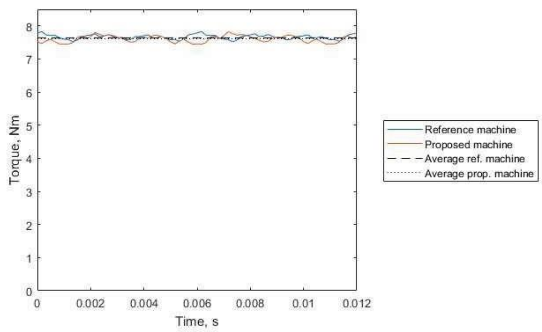

Fig 14. Torque comparison between the IPMSM and the PMaSynRM

VI. Conclusion

IPMSM which are used as power steering motors in the automotive industry produce their DC magnetic field with rare earth permanent magnets. Due to the increasing value of this type of magnets there is a need of a reduction or a replacement with ferrite magnets. In this paper it is described an effort for minimizing the magnet's volume of a 12 slot 10 pole power steering motor. The proposed rotor consists of 4 poles because this configuration has the advantage of exhibiting reluctance torque. In addition, the active length of the machine has been increased by 42% to enhance the torque production. It is clear that the rated torque of the reference machine can be reached when less magnets are used. The problem of torque pulsation has also been addressed. Stator skewing has been employed so the torque ripple content of the proposed rotor can meet the requirements of the specific application.

References

[1] J. Baek, S. Kwak, and H. A. Toliyat, "Optimal Design and Performance Analysis of Permanent Magnet Assisted Synchronous Reluctance Portable Generators," *Journal of Magnetics*, vol. 18, no. 1. The Korean Magnetics Society, pp. 65–73, 31-Mar-2013.

[2] https://eitrawmaterials.eu/wp-content/uploads/2021/09/ERMA-Action-Plan-2021-A-European-Call-for-Action.pdf

[3] M. Barcaro, N. Bianchi and F. Magnussen, "Permanent-Magnet Optimization in Permanent-Magnet-Assisted Synchronous Reluctance Motor for a Wide Constant-Power Speed Range," in *IEEE Transactions on Industrial Electronics*, vol. 59, no. 6, pp. 2495-2502, June 2012, doi: 10.1109/TIE.2011.2167731.

[4] P. P. Florin, R. Mircea, P. Adrian-Cornel, R. Martis and C. Martis, "Comparative Analysis for an Electric Power Steering System," *2018 XIII International Conference on Electrical Machines (ICEM)*, 2018, pp. 590-596, doi: 10.1109/ICELMACH.2018.8507038.

[5] Florin-Adelin Pop-Pîgleșan, "Synchronous Reluctance Machine for automotive applications", pp. 67

[6] Huynh, Thanh Anh & Hsieh, Min-Fu & Shih, Kai-Jung & Kuo, Hsiu-Fu. (2018). An Investigation into the Effect of PM Arrangements on PMa-SynRM Performance. IEEE Transactions on Industry Applications. PP. 1-1. 10.1109/TIA.2018.2853042.

[7] Jung-Ho Lee, Young-Jin Jang (2005). Characteristic analysis of permanent magnet-assisted synchronous reluctance motor for high power application. Journal of Applied Physics 97, 10Q503.

[8] Neodymium magnet - Wikipedia

[9] Ferrite Magnets - Bunting - eMagnets (e-magnetsuk.com)

[10] Viego, Percy & Gómez Sarduy, Julio & Yanes, José & Quispe, Enrique & Santos, Vladimir. (2021). Reducing torque pulsations in PMa-SynRM: a way for improving motor performance. International Journal of Power Electronics and Drive Systems. 12. 67-79. 10.11591/ijpeds.v12.i1.pp67-79.

[11] Bianchi, N. & Bolognani, Silverio & Bon, Diego & Pre, Michele. (2009). Rotor Flux-Barrier Design for Torque Ripple Reduction in Synchronous Reluctance and PM-Assisted Synchronous Reluctance Motors. Industry Applications, IEEE Transactions on. 45. 921 - 928. 10.1109/TIA.2009.2018960.

[12] Briggner, V. (2018). Design and comparison of PMaSynRM versus PMSM for pumping applications (Dissertation). Retrieved from http://urn.kb.se/resolve?urn=urn:nbn:se:kth:diva-235279

[13] Wu Ren, Qiang Xu, Qiong Li and Le Chen, "Reducing cogging torque and suppressing torque ripple in PMASynRM for EV/HEV applications, "*2014 IEEE Conference and Expo Transportation Electrification Asia-Pacific (ITEC Asia-Pacific)*, 2014, pp. 1-6, doi: 10.1109/ITEC-AP.2014.6940852.

[14] Bahrim, Fatihah Shafiqah & Sulaiman, Erwan & Jusoh, Laili & Omar, Mohd Fairoz & Kumar, Rajesh. (2017). Cogging Torque Reduction of IPM Motor using Skewing, Notching, Pole Pairing and Rotor Pole Axial Pairing. International Journal of Applied Engineering Research. 12. 1371-1376.

[15] Y. Jeong, K. Kim, Y. Kim, B. Park and S. Jung, "Design characteristics of PMa-SynRM and performance comparison with IPMSM based on numerical analysis," 2012 XXth International Conference on Electrical Machines, 2012, pp. 164-170, doi: 10.1109/ICElMach.2012.6349858.